Asian Journal of Advances in Medical Science

3(1): 179-192, 2021

SYNTHESIS AND IN-SILICO ANTI-INFLAMMATORY INVESTIGATION OF 2, 3-DIHYDROCHROMEN-4-ONE AND 3, 4-DIHYDROBENZO[B]OXEPIN-5(2H)-ONE BASED PYRAZOLE DERIVATIVES

C. JEYSIHA[1], D. ABILASA[1], G. REXIN THUSNAVIS[1], R. SUBRAMANIAN[2] AND P. PALANISAMY[1*]

[1]Department of Chemistry, Pioneer Kumaraswamy College, Nagercoil, Tamilnadu, India.
[2]Department of Chemistry, M. S. University College, Govinthaperi, Tamilnadu, India.

AUTHORS' CONTRIBUTIONS

This work was carried out in collaboration among all authors. All authors read and approved the final manuscript.

Received: 05 May 2021
Accepted: 10 July 2021
Published: 14 July 2021

Original Research Article

ABSTRACT

This study synthesized six pyrazole derivatives from the key intermediates 2,3-dihydrochromen-4-one and 3,4-dihydrobenzo[b]oxepin-5(2H)-one. We have characterized all pyrazole derivatives as well as conducted *in silico* anti-inflammatory studies. The DFT calculations were performed using Gaussian 09 software. The compound **9** has the lowest energy gap (ΔE, 1.0698 eV), lowest hardness (0.5349 eV), highest softness (1.8695 eV), and highest electrophilicity (7.0809eV) among all pyrazole derivatives and standard Aspirin. Swiss ADME software was used to carry out the ADME analysis. The chloro-substituted pyrazole derivatives (**5**, **6**, and **9**) were non-toxic, however, the nitrogen-substituted pyrazole derivatives (**10**, **13** and **14**) and Aspirin were toxic. The docking patterns of the pyrazole derivatives with COX-2 selective inhibitors proteins (**5F19**) have been studied. Compound **9** has the lower binding energy (-10.2Kcal/mol) as compared with that of other pyrazole derivatives and standard Aspirin drugs. As a result, the pyrazole derivatives compound 9 is a promising anti-inflammatory drug with selective COX-2 inhibition as compared to the Aspirin drugs physicochemical properties.

Keywords: Pyrazole derivatives; docking study; ADMET; DFT studies and anti-inflammatory activity.

1. INTRODUCTION

Pyrazoles are five-membered heterocycles which are widely used for organic synthesis. Various structures contain the pyrazole nucleus, which has numerous applications in the fields of technology, medicine, agriculture, and biochemistry [1,2]. Currently, pyrazole systems are gaining attention due to their remarkable pharmacological properties [3-5]. A new class of pyrazole derivatives was evaluated as selective cyclooxygenase-2 inhibitors (COX-2) [6,7]. Bekhit et al. have synthesized a series of novel synthetic pyrazolyl benzenesulfonamide derivatives bearing thiazolyl ring and evaluated their anti-inflammatory properties [8]. Girisha et al., [9] synthesized and evaluated a new series of 1-acetyl/propyl-3-aryl-5-(5-chloro-3-methyl-1-phenyl-1H-pyrazol-4-yl)-2-pyrazolines for their analgesic and anti-inflammatory effects. El-Moghazy et al., [10] have synthesized a novel series of pyrazoles that

**Corresponding author: Email: ppschem08@gmail.com, palanisamypandaram78@gmail.com;*

includes benzenesulfonamides and tested them in vivo for anti-inflammatory activity. Several new 1H-pyrazole-4-acetates possessing quinazoline ring were synthesized and investigated for analgesic and anti-inflammatory activity [11]. A number of new 1,3,4-trisubstituted pyrazoles have been synthesized and tested for analgesic and anti-inflammatory activity [12].

In-Silico drug design system uses several important principles to estimate newly calculated molecules, such as Molecular docking, non-bonding interactions, and ADMET. [13,14]. Non-steroidal anti-inflammatory drugs (NSAIDs) are frequently used in treating arthritis, fever, and pain by inhibiting the production of prostaglandins via the cyclooxygenase (COX) enzyme pathway [15,16]. A COX-2 enzyme is one of the key players in prostaglandin synthesis, prostacyclin synthesis, and thromboxane synthesis within cells, therefore, suppressing this enzyme activity may have therapeutic benefits [17-19]. Based on the above apparent evidence, and as part of our interest in the Synthesis of 3,4-dihydrobenzo[b]oxepin-5(2H)-one Based Pyrazole derivatives, we conducted in silico anti-inflammatory studies.

2. MATERIALS AND METHODS

2. 1 General Comments

FT IR spectra were recorded on JASCO FT-IR Model 410 spectrophotometer. The evaluating was performed in the 4000-400 cm^{-1} wave number range. ^{1}H-NMR spectra were recorded on a 400 MHz Varian spectrometer using $CDCl_3$ solvent system. Chemicals were purchased commercially and used as such. TLC plates prepared from silica gel (Merck) grade were used to monitor each reaction. The products formed were purified by fluid bed column chromatography using silica gel, 60-120 mesh (Merck).

2.2 Synthesis

2. 2.1 Synthesis of pyrazole derivatives

The Claisen-Smith condensation reaction between 2,3-dihydrochromen-4-one and 3,4-dihydrobenzo[b]oxepin-5(2H)-one with appropriate aldehydes to give compounds **3**, **4**, **8**, **11**, and **12**. The compounds were treated with phenyl hydrazine hydrochloride (0.01 mol) in 30 ml ethanol for 12 h, then the excess solvent was removed under reduced pressure and the reaction mixture was poured into crushed ice. When the solid mass was filtered, dried, and recrystallized with ethanol, the compounds **5, 6**, **9**, **10**, **13** and **14** were obtained.

2.3 DFT Studies on Compounds 5, 6, 9, 10, 13, and 14

The properties of molecular structures were investigated using density functional theory (DFT) using B3LYP/6-31G (d,p), using the Gaussian 09 program [20]. Calculations of the Ionization potential (IP), electron affinities (EA), electronegativity (χ), chemical potential (μ) global hardness (η), global softness (σ), and electrophilicity index (ω) were performed by utilizing the following equations [21]:

$$IP = – EHOMO \quad (1)$$

$$EA = –ELUMO \quad (2)$$

$$\eta = ELUMO – EHOMO \quad (3)$$

$$\sigma = 1 / \eta \quad (4)$$

$$\chi = – (EHOMO – ELUMO) / 2 \quad (5)$$

$$\mu = (EHOMO – ELUMO) / 2 \quad (6)$$

$$\omega = \mu 2 / 2 \eta \quad (7)$$

2.4 ADMET Predictions

In drug discovery, computational models are used to predict absorption, distribution, metabolism, excretion, and toxicity (ADMET), which protects investment and time. Based on the ADMET SAR online database, aspirin and pyrazole derivatives were predicted to display ADMET properties [22]. The Swiss ADME online software predicts ADME parameters, pharmacokinetic properties, drug similarity, and medicinal chemistry properties of compounds. The Swiss ADME server was opened, and the structures were drawn, then they were converted to SMILES, then the run button was clicked, and results were presented [23].

2.5 Docking Studies of Compounds 5, 6, 9, 10, 13, and 14 on 5F19 Proteins

A molecular docking simulation was performed to investigate the mechanism of prostaglandin H2 (PGH2) inhibition by newly designed Pyrazole derivatives and their binding affinity and mode(s) with target proteins [24. Human cyclooxygenase-2 (PDB ID: 5F19) has been analyzed in 3D by protein data bank (PDB) database using the PDB file format [25]. PyMol (version 1.3) software packages were used to eliminate hetero atoms and water molecules [26]. A molecular docking study was carried out on the optimized drugs up against the human prostaglandin synthase protein (5F19). We performed

molecular docking simulations with Auto Dock software by treating the protein as a macromolecule and the drug as a ligand. During docking, both protein and ligand structures were stored in the pdbqt format required by Accelrys Discovery Studio (version 4.1) to analyze and visualize the docking result and search for interactions between ligands and target proteins [27,28].

3. RESULTS AND DISCUSSION

The six pyrazole derivatives described in reaction sequence for the synthesis are summarized in Scheme 1. 2,3-dihydrochromen-4-one/ 3,4-dihydrobenzo[b]oxepin-5(2H)-one (0.01 mol) and appropriate aromatic aldehydes (0.01 mol) are mixed at room temperature in diluted ethanolic sodium hydroxide solution to give the Claisen Schmidt condensation product. Subsequently, Claisen Schmidt condensation product was treated with appropriate substituted phenyl hydrazine hydrochloride to yield pyrazole derivatives. The yields of the pyrazole derivatives ranged from 58% to 68% after recrystallization with absolute ethanol. We checked the purity of the compounds by TLC using eluant ethanol: chloroform (8:2) and elemental analysis. Both the analytic and spectral data corresponded to the suggested structures for all synthesized compounds.

The solid mass was filtered dried and recrystallized with ethanol gave the 3-(4-chlorophenyl)-2,3,3a,4-tetrahydro-2-phenylchromeno[4,3-c] pyrazole (**5**).The IR (KBr) (Fig. 1) spectrum of **5** afforded pyrazoline C=N stretching at 1583 cm^{-1}, Ar-N stretching at 1283 cm^{-1}, N-N-C stretching at 1199cm^{-1} and C-N stretching at 1083 cm^{-1}. The ^{1}H-NMR ($CDCl_3$) spectrum showed a multiplet at δ 2.4 ppm (CH-C<u>H</u>-CH_2), two doublets at δ 2.9 (CH-CH-C<u>H</u>$_2$) and δ 3.9 (C<u>H</u>-CH-CH_2), a multiplet in the region at δ6.8-7.5 ppm (aromatic protons). The solid mass was filtered dried and recrystallized with ethanol gave the 3-(2-chlorophenyl)-2,3,3a,4-tetrahydro-2-phenylchromeno[4,3-c] pyrazole (**9**). The IR (KBr) spectrum of **5** afforded pyrazoline C=N stretching at 1576 cm^{-1}, Ar-N stretching at 1293 cm^{-1}, N-N-C stretching at 1206cm^{-1} and C-N stretching at 1068 cm^{-1}. The ^{1}H-NMR ($CDCl_3$) spectrum showed a multiplet at δ 2.5 ppm (CH-C<u>H</u>-CH_2), two doublets at δ 2.8 (CH-CH-C<u>H</u>$_2$) and δ 3.9 (C<u>H</u>-CH-CH_2), a multiplet in the region at δ6.9-7.6 ppm (aromatic protons).

The solid mass was filtered dried and recrystallized with ethanol gave the 3-(4-nitrophenyl)-2,3,3a,4-tetrahydro-2-phenylchromeno[4,3-c]pyrazole (**13**).The IR (KBr) spectrum of **5** afforded pyrazoline C=N stretching at 1598 cm^{-1}, Ar-N stretching at 1311 cm^{-1}, N-N-C stretching at 1214cm^{-1} and C-N stretching at 1116 cm^{-1}. The ^{1}H-NMR ($CDCl_3$) spectrum showed a multiplet at δ 2.5 ppm (CH-C<u>H</u>-CH_2), two doublets at δ 2.9 (CH-CH-C<u>H</u>$_2$) and δ 3.8 (C<u>H</u>-CH-CH_2), a multiplet in the region at δ7.7-8.2 ppm (aromatic protons). The solid mass was filtered dried and recrystallized with ethanol gave the 3-(4-chlorophenyl)-2-phenyl-3,3a,4,5-tetrahydro-2H-[1] benzoxepino[5,4-c]pyrazole (**6**).The IR (KBr) spectrum of **5** afforded pyrazoline C=N stretching at 1603 cm^{-1}, Ar-N stretching at 1305 cm^{-1}, N-N-C stretching at 1206cm^{-1} and C-N stretching at 1104 cm^{-1}. The ^{1}H-NMR ($CDCl_3$) spectrum showed a two multiplets at δ 1.8 ppm (S-CH_2-C<u>H</u>$_2$) and 2.1 (CH_2-CH_2-C<u>H</u>), a triplet at δ 2.9 (S-C<u>H</u>$_2$-CH_2), a doublet at δ 3.9 (CH_2-CH-C<u>H</u>), a multiplet in the region at δ6.8-7.6 ppm (aromatic protons).

The solid mass was filtered dried and recrystallized with ethanol gave the 3-(2-chlorophenyl)-2-phenyl-3,3a,4,5-tetrahydro-2H-[1]benzothiepino[5,4-c]pyrazole (**10**).The IR (KBr) spectrum of **5** afforded pyrazoline C=N stretching at 1608 cm^{-1}, Ar-N stretching at 1301 cm^{-1}, N-N-C stretching at 1208cm^{-1} and C-N stretching at1112 cm^{-1}. The ^{1}H-NMR ($CDCl_3$) spectrum showed a two multiplet at δ 1.7 ppm (S-CH_2-C<u>H</u>$_2$) and 2.0 (CH_2-CH_2-C<u>H</u>), a triplet at δ 2.8 (S-C<u>H</u>$_2$-CH_2), a doublet at δ 3.8 (CH_2-CH-C<u>H</u>), a multiplet in the region at δ6.5-7.6 ppm (aromatic protons). The solid mass was filtered dried and recrystallized with ethanol gave the 3-(-nitrorophenyl)-2-phenyl-3,3a,4,5-tetrahydro-2H-[1]benzoxepino[5,4-c]pyrazole (**14**).The IR (KBr) spectrum of **5** afforded pyrazoline C=N stretching at 1603 cm^{-1}, Ar-N stretching at 1305 cm^{-1}, N-N-C stretching at 1206cm^{-1} and C-N stretching at 1104 cm^{-1}. The ^{1}H-NMR ($CDCl_3$) spectrum showed a two multiplet at δ 1.9 ppm (S-CH_2-C<u>H</u>$_2$) and 2.2 (CH_2-CH_2-C<u>H</u>), a triplet at δ 3.0 (S-C<u>H</u>$_2$-CH_2), a doublet at δ 4.0 (CH_2-CH-C<u>H</u>), a multiplet in the region at δ7.2-7.7 ppm (aromatic protons).

3. 1 DFT Studies

As shown in Fig. 1, the gas phase geometrical parameters for the optimized structures of compounds 5, 6, 9, 10, 13, and Aspirin at the DFT/3-21G(d) level. The DFT method has been used to investigate the electronic structures of 5, 6, 9, 10, 13, 14, and Aspirin. The optimized diagram in Fig. 1 shows the structures of pyrazole derivatives 5, 6, 9, 10, 13, 14 and Standard Aspirin respectively. As a result of the inverse relationship between stabilization energy and orbital energy difference, terms involving the frontier molecular orbitals (FMO) could provide dominating contributions. HOMO-LUMO energy gap, molecular hardness, ionization energy, electron affinity, and

total energy are very important physical parameters for the chemical reactivity and biological activities of the compounds under study. E_{HOMO} is often associated with the electron donating ability of a molecule; high values of E_{HOMO} may indicate that that molecule donates electrons to appropriate acceptor molecules with lower energy MO. On the other hand, ELUMO refers to the ability of the molecule to accept electrons [29].

The binding ability of the molecule increases with increasing HOMO energy value and decreases with decreasing LUMO energy value. Thus, the lower the value of ELUMO, the more probable it is that the molecule will accept electrons. Fig. 1 shows the optimized structures of pyrazole derivatives 5, 6, 9, 10, 13, 14, and aspirin. Furthermore, the gap between the HOMO and LUMO energy levels of the molecule (ΔE) is an important parameter determining the reactivity of the molecule. The decrease in ΔE (especially for the cationic species) leads to an increase in the reactivity, which reduces the stability of the molecule. Absolute hardness, η, and softness, σ, are important properties to determine a molecule's stability and reactivity. Hard molecules have a large energy gap, while soft molecules have a small one. Soft molecules are more reactive than hard ones because they can readily accept electrons from an acceptor. In the simple transfer of electrons, adsorption could occur at the part of the molecule where σ has the highest magnitude whereas η has the lowest [30]. The electrophilicity, ω, measures the electrophilic power of a molecule. It has been shown that the higher the value of X, the less capable a molecule is of donating electrons [31].

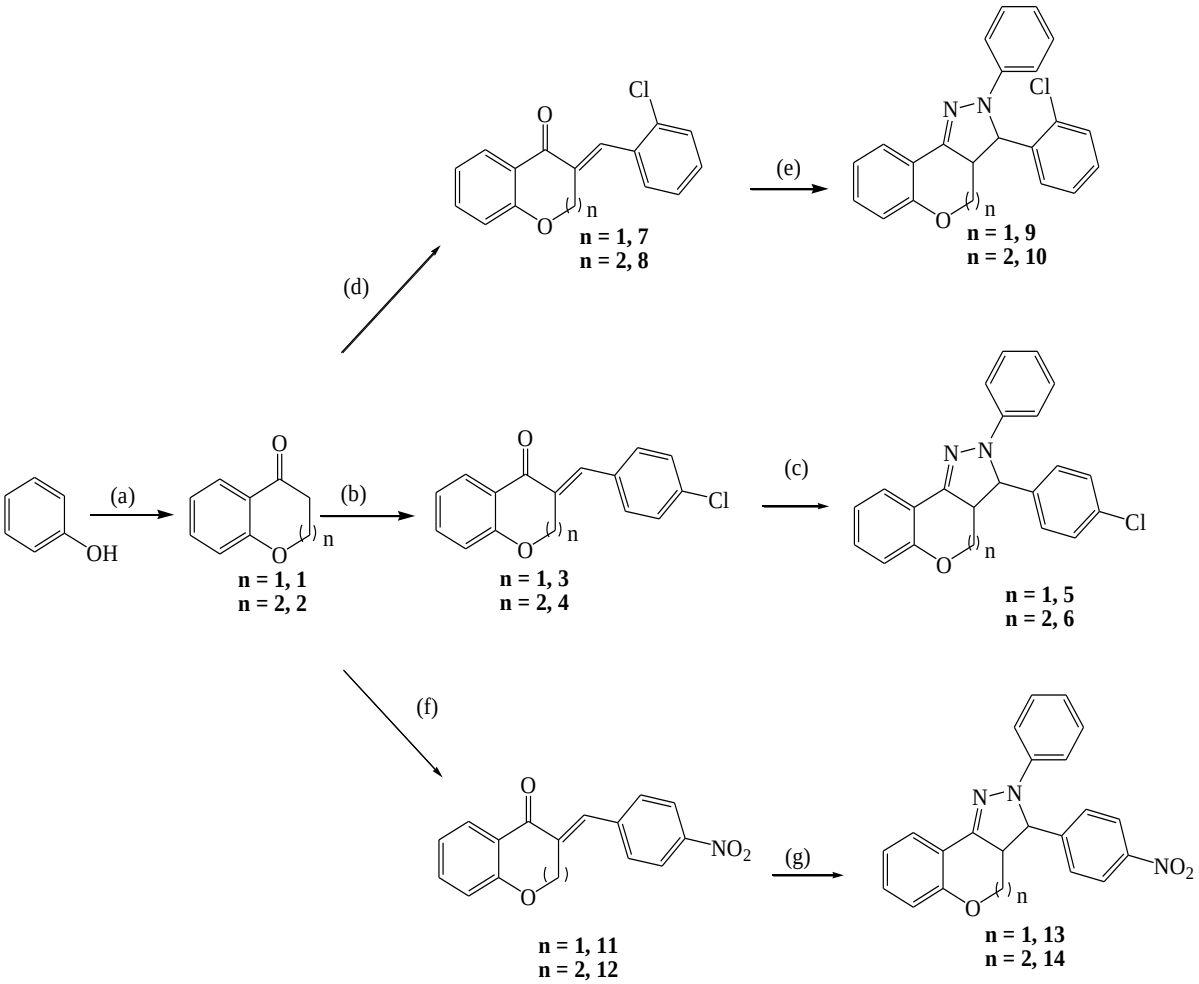

Scheme 1. Protocol for the synthesis of pyrazole derivatives based on 2,3-dihydrochromen-4-one and 3,4-dihydrobenzo[b]oxepin-5(2H)-one, Reaction and Conditions:(a) $ClCH_2COOH/NaOH/ClCH_2CH_2COOH/NaOH$; PPA (b) Na, dry EtOH,p-chlorobenzaldehyde (c) $C_6H_5NHNH_2.HCl$, CH_3COOH (d) Na, dry EtOH,o-chlorobenzaldehyde (e) $C_6H_5NHNH_2.HCl$, CH_3COOH (f) Na, dry EtOH,p- nitrobenzaldehyde (g) $C_6H_5NHNH_2.HCl$, CH_3COOH

Table 1. DFT results of 5, 6, 9, 10, 13, 14, and aspirin

Compound	HOMO	LUMO	Energy gap potential (IP)	Ionisation potential(μ)	Electrochemical	Hardness(η)	Softness(σ)	Electrophilicity(ω)
5	-3.2463	-1.4441	1.8022	3.2463	-2.3452	0.9011	1.1098	3.0518
6	-5.3774	-2.2508	3.1266	5.3774	-3.8141	1.5633	0.6397	4.6528
9	-3.2872	-2.2174	1.0698	3.2872	-2.7523	0.5349	1.8695	7.0809
10	-4.0991	-1.6724	2.4267	4.0991	-2.8857	1.2134	0.8242	3.4316
13	-5.4067	-1.5545	3.8522	5.4067	-3.4806	1.9261	0.5192	3.1448
14	-5.2114	-2.2549	2.9565	5.2114	-3.7332	1.4783	0.6765	4.7138
Aspirin	-6.7750	-1.4754	5.2996	6.7750	-4.1252	2.6498	0.3774	3.2111

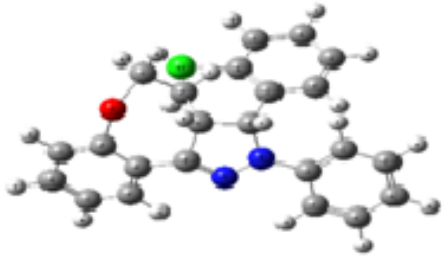

5a

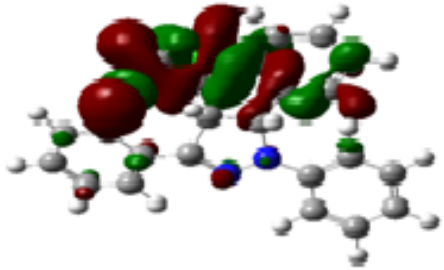

5b

5c

6a

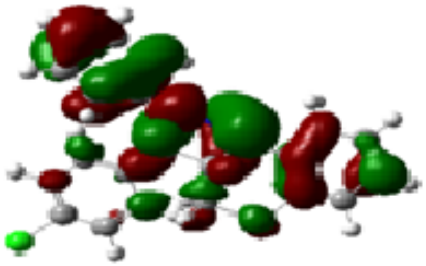

6b

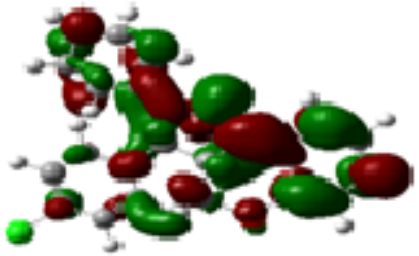

6c

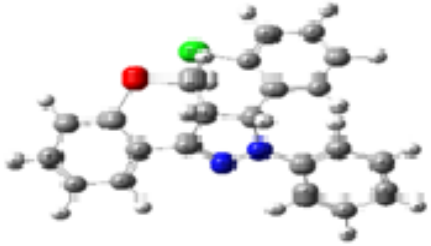

9a

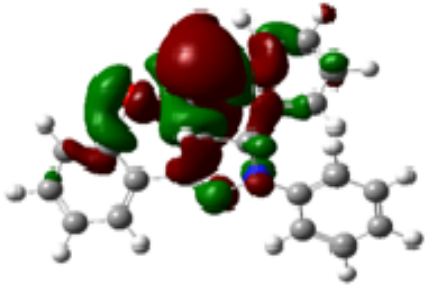

9b

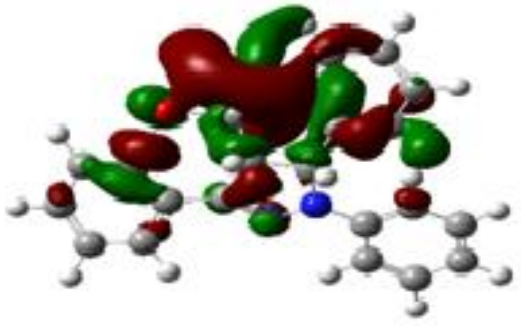

9c

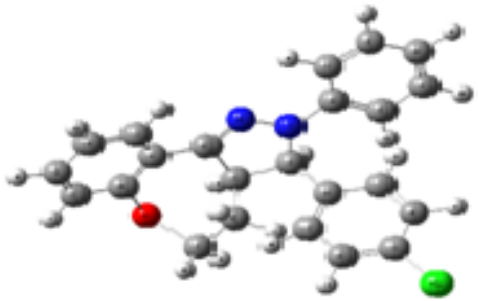

10a

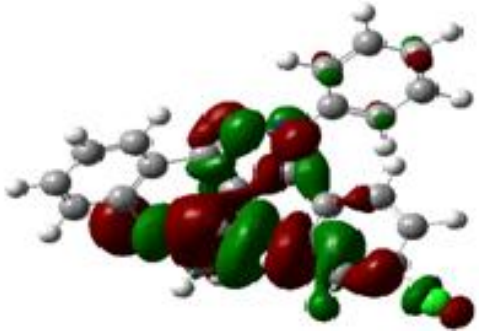

10b

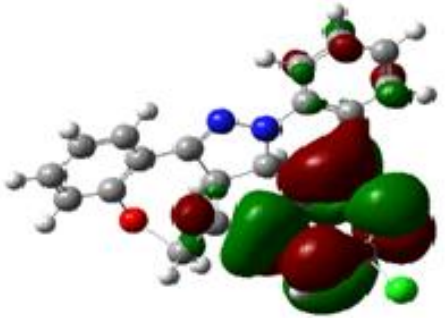

10c

13a

13b

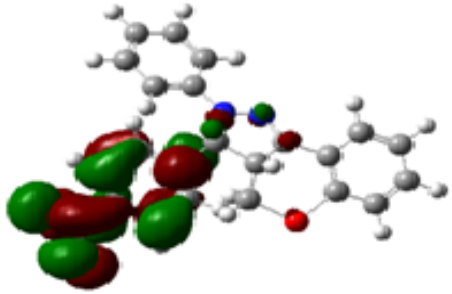

13c

14a

14b

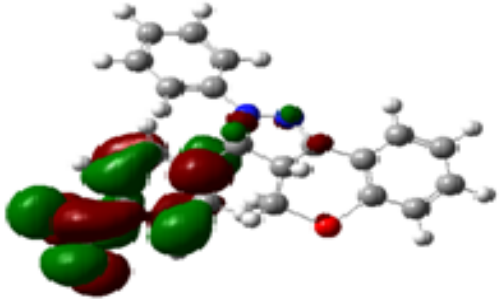

14c

Aspirin a Aspirin b Aspirin c

Fig. 1. a) DFT-Optimized structure b) DFT- HOMO Structure c) DFT- LUMO Structure of 5, 6, 9, 10, 13, 14, and Aspirin 3. 2 ADMET analysis

Table 2. Physicochemical properties of 5, 6, 9, 10, 13,14, and aspirin

Compound	Formula	Molecular weight (g/mol)	Number of heavy atoms	Number of rotatable bonds	Number of H-bond acceptors	Topological polar surface Area(Å²)
5	$C_{22}H_{17}ClN_2O$	360.84	26	2	2	24.83
6	$C_{23}H_{19}ClN_2O$	374.86	27	2	2	24.83
9	$C_{22}H_{17}ClN_2O$	360.84	26	2	2	24.83
10	$C_{23}H_{19}ClN_2O$	374.86	27	2	2	24.83
13	$C_{22}H_{17}N_3O_3$	371.39	28	3	4	70.65
14	$C_{23}H_{19}N_3O_3$	385.42	29	3	4	70.65
Aspirin	$C_9H_8O_4$	180.16	13	3	4	63.60

Table 3. Pharmacokinetics of 5, 6, 9, 10, 13, 14 and aspirin

Compound	GI absorption	Blood Brain Barrier (BBB)	CYP1A2 inhibitor	CYP2C19 inhibitor	CYP2C9 inhibitor	Drug likeness	Log Kp skin permeation cm/s	Acute oral toxicity
5	High	Yes	Yes	Yes	Yes	Yes	-4.65	Non-Toxic(-)
6	High	Yes	Yes	Yes	Yes	Yes	-4.48	Non-Toxic(-)
9	High	Yes	Yes	Yes	Yes	Yes	-4.65	Non-Toxic(-)
10	High	Yes	Yes	Yes	Yes	Yes	-4.48	Toxic(+)
13	High	Yes	No	Yes	Yes	Yes	-5.28	Toxic(+)
14	High	Yes	No	Yes	Yes	Yes	-5.11	Toxic(+)
Aspirin	High	Yes	No	No	No	Yes	-6.55	Toxic(+)

As compared with the Standard Aspirin, all synthesized pyrazole derivatives 5, 6, 9, 10, 13, and 14 have the lowest energy gap, lowest hardness, highest softness, and highest electrophilicity. Thus, all pyrazole compounds are more potent and chemically reactive than Standard Aspirin. Similarly, 2,3-dihydrochromen-4-one pyrazole derivatives (**5, 6,** and **9**) are more active than those of 3,4-dihydrobenzo[b]oxepin-5(2H)-one pyrazole derivatives (**10, 13,** and **14**). Compound 9 has the lowest energy gap (ΔE, 1.0698 eV), lowest hardness (0.5349 eV), highest softness (1.8695 eV), and highest electrophilicity (7.0809eV) of the other pyrazole derivatives 5, 6, 10, 13, and 14 as well as standard Aspirin.

We conducted ADME analysis and cardio toxicity analysis in Swiss ADME software. We calculated ADMET levels in order to analyze the safety level of human analogues after administration. The predictions for passive human gastrointestinal absorption (HIA) and blood-brain barrier permeation (BBB) are based on the BOILED-Egg mode. The graphical classification model can be displayed on the Swiss ADME result page by clicking the red button below the sketcher once all input molecules have been processed. Other binary classification models are also included, which are based on the propensity of a given small molecule to act as a substrate or inhibitor of certain proteins governing important pharmacokinetic behaviors [32,33]. It is also essential to know how molecules interact with cytochromes P450 (CYP). This superfamily of isoenzymes is critical to drug elimination through metabolic biotransformation [34]. It has been suggested that CYP and P-gp can process small molecules synergistically to improve protection of tissues and organisms [35]. One can estimate that 50 to 90% (depending on the authors) of therapeutic molecules are substrate of five major isoforms (CYP1A2, CYP2C19, CYP2C9, CYP2D6, CYP3A4) [36]. Inhibition of these isoenzymes is certainly one major cause of pharmacokinetics-related drug-drug interactions [37,38]. Table 2 shows Physicochemical Properties, and Table 3 shows Pharmacokinetics Properties. Pyrazole derivatives and Aspirin showed high gut absorption, blood-brain barrier (BBB) and drug like properties in the Swiss ADME section. The Swiss ADME section allows defining drug likeness using five different rule-based filters. Major pharmaceutical companies often use these filters to refine their proprietary chemical collections. The Lipinski (Pfizer) filter is the pioneer rule-of-five implemented [39] (Lipinski et al.,2001). The Ghose (Amgen), Veber (GSK), Egan (Pharmacia) and Muegge (Bayer) methods were adapted from refs [40-43], respectively. 2,3-dihydrochromen-4-one pyrazole derivatives (**5, 6,** and **9**) and 3,4-dihydrobenzo[b]oxepin-5(2H)-one pyrazole derivatives (**10, 13,** and **14**) have been implicated in CYP2C19 and CYP2C9 inhibition, respectively, but Aspirin is not involved with these inhibitors. Pyrazole derivatives (5, 6, 9, and 10) and aspirin are CYP1A2 inhibitors, but not the Nitro substituted pyrazole derivatives (13 and 14). Nitro-substituted pyrazole derivatives (0, 10, 13, and 14) showed toxic properties, while chloro- substituted pyrazole derivatives (5, 6, and 9) showed non-toxic properties.

3.3 Docking Studies of Compounds 5, 6, 9, 10, 13, and 14 on 5F19 Protein

An analysis of docking was carried out using COX protein 5F19. By using AutoDock tools, hydrogen atoms, atomic types and salvation parameters were added to the model [44]. Calculations of the van der Walls term and the electrostatic term were performed using parameter set- and distance-dependent dielectric functions in AUTODOCK.. As shown in Table 4, the binding energies of compounds 5, 6, 9, 10, 13, and 14 can be calculated.

Table 4. Binding energy of compounds 5, 6, 9, 10, 13, 14 and aspirin with 5F19 protein

Compound	Binding energy (k.cal)
5	-8.26
6	-8.11
9	-10.2
10	-9.64
13	-7.84
14	-6.59
Aspirin	-5.6

A greater negative value of binding affinity indicates a stronger interaction between drugs and the receptor protein. Strong hydrogen bonds are a major element contributing to increased binding affinity of drugs with the receptor protein [45]. All pyrazole derivatives (5, 6, 9, 10, 13, and 14) showed the greater negative values of binding affinity compared to Aspirin in the docking analysis. Among the chloro-substituted pyrazoles (5, 6, and 9) there is less spontaneous binding than among the Nitro-substituted pyrazoles (10, 13, and 14). A lower binding energy appears to be associated with compound 9 (-10.2Kcal / mol) compared to the binding energy of the other pyrazole derivatives. As a result, compound 9 is the most effective anti-inflammatory compound with COX protein (5F19) compared to the rest of the derivatives and aspirin drugs.

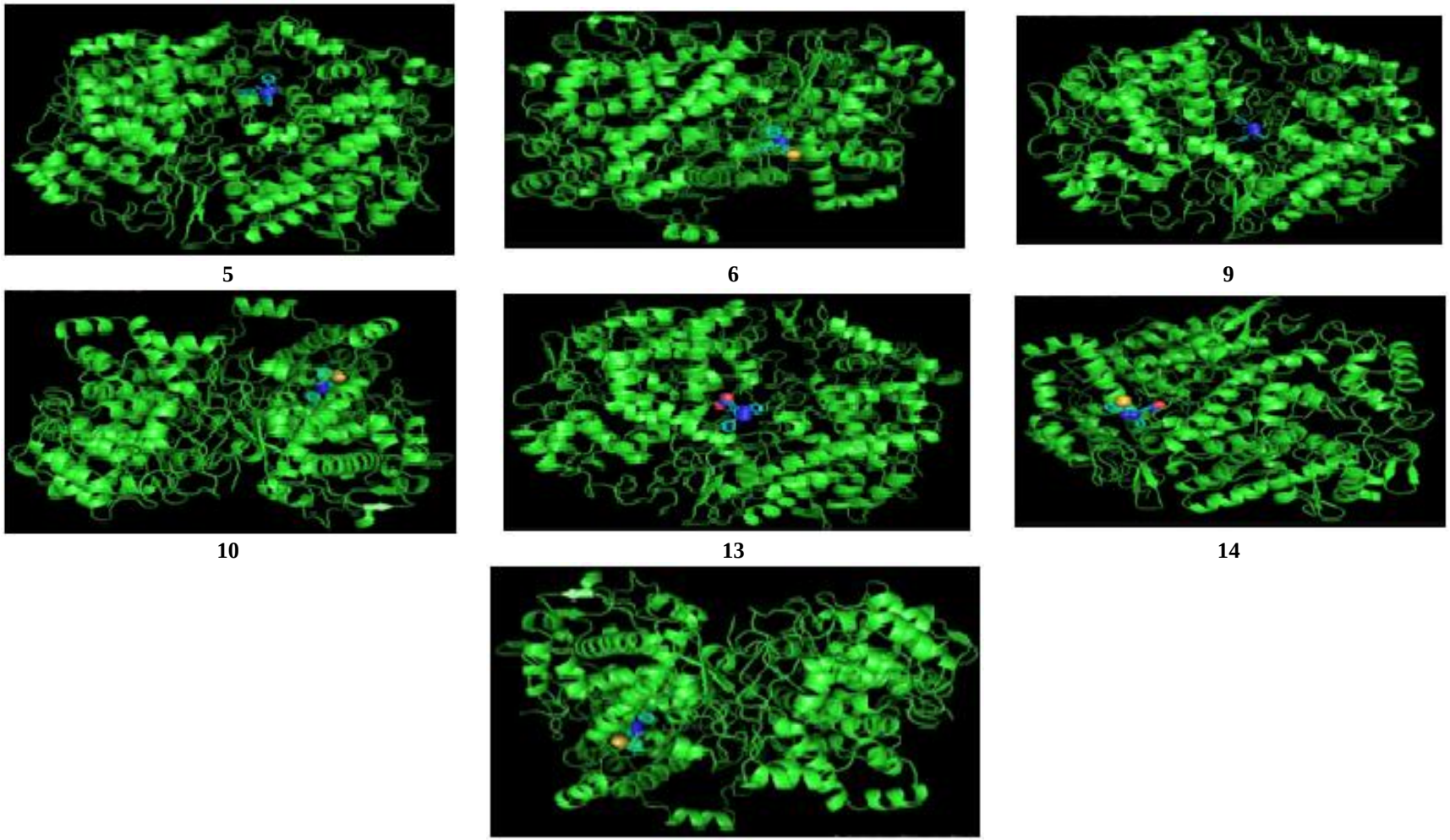

Fig. 2. Different binding sites of compounds in docking studies

4. CONCLUSION

In silico anti-inflammatory investigation has been completed on the six pyrazole derivatives starting from 2,3-dihydrochromen-4-one and 3,4-dihydrobenzo[b]oxepin-5(2H)-one. Compound **9** has the lowest energy gap (ΔE, 1.0698 eV), lowest hardness (0.5349 eV), highest softness (1.8695 eV), and highest electrophilicity (7.0809eV) than the other pyrazole derivatives and standard Aspirin. Nitro-substituted pyrazole derivatives (10, 13, and 14) showed toxic properties, while chloro- substituted pyrazole derivatives (5, 6, and 9) showed non-toxic properties. Based on docking results, compound 9 has a lower binding energy (-10.1Kcal / mol) compared to other pyrazole derivatives. According to the above results, pyrazole derivative compound **9** had the best anti-inflammatory effect on the COX protein (5F19) in comparison to all of the other derivatives as well as aspirin.

CONSENT

It is not applicable.

ETHICAL APPROVAL

It is not applicable.

COMPETING INTERESTS

Authors have declared that no competing interests exist.

REFERENCES

1. Ansari A, Ali A, Asif M. Biologically active pyrazole derivatives. New J. Chem. 2017;41: 16–41.
2. Fustero S, Sánchez-Roselló M, Barrio P, Simón-Fuentes A. From 2000 to Mid-2010: A fruitful decade for the synthesis of pyrazoles. Chem. Rev. 2011;111:6984–7034.
3. Steinbach G Lynch, Robin PM, Wallace KSP, Hawk MH, Gordon E, Wakabayashi GB, et al. The effect of celecoxib, a cyclooxygenase-2 inhibitor, in familial adenomatous polyposis. N. Engl. J. Med. 2000; 342:1946–1952.
4. Uslaner JM, Parmentier-Batteur S, Flick RB, Surles NO, Lam JS. McNaughton C.H. Dose-dependent effect of CDPPB, the mGluR5 positive allosteric modulator, on recognition memory is associated with GluR1 and CREB phosphorylation in the prefrontal cortex and hippocampus. Neuropharmacology. 2009;57: 531–538.
5. Ghaneya SH, Doaa EAR, Esraa AA, Rana H, Refaey MA, Yassin MN. New pyrazole derivatives: Synthesis, anti-inflammatory activity, cycloxygenase inhibition assay and evaluation of mPGES. Eur. J. Med. Chem. 2019;171:332-342.
6. Kamble RD, Meshram RJ, Hese SV, More RA, Kamble SS, Gacche RN, Dawane BS. Synthesis and in silico investigation of thiazoles bearing pyrazoles derivatives as anti-inflammatory agents. Comput. Biol. Chem. 2016;61:86–96.
7. Namera DL. Thakkar SS, Thakor P, Umed B, Shah A. Arylidene analogues as selective COX-2 inhibitors: Synthesis, characterization, in-silico and in vitro studies, Journal of Biomolecular Structure and Dynamics; 2020. DOI: 10.1080/07391102.2020.1806109
8. Bekhit AA, Ashour HMA, Abdel Ghany YS, Bekhit AA, Baraka A. Synthesis and biological evaluation of some thiazolyl and thiadiazolyl derivatives of 1*H*-pyrazole as anti-inflammatory antimicrobial agents. Eur. J. Med. Chem. 2008;43:456–463.
9. Girisha KS, Kalluraya B, Narayana V, Padmashree V. Synthesis and pharmacological study of 1-acetyl/propyl-3-aryl-5-(5-chloro-3-methyl-1-phenyl-1*H*-pyrazol-4-yl)-2-pyrazoline. Eur. J. Med. Chem. 2010;45:4640–4644.
10. El-Moghazy SM, Barsoum FF, Abdel-Rahman HM, Marzouk AA. Synthesis and anti-inflammatory activity of some pyrazole derivatives. Med. Chem. Res. 2012;21:1722–1733.
11. Maggio B, Daidone G, Raffa D, Plescia S, Mantione L, Cutuli VMC, et al. Synthesis and pharmacological study of ethyl 1-methyl-5-(substituted 3,4-dihydro-4-oxoquinazolin-3-yl)-1*H*-pyrazole-4-acetates. Eur. J. Med. Chem. 2001;36:737–742.
12. Vijesh AM, Isloor AM, Shetty P, Sundershan S, Fun HK. New pyrazole derivatives containing 1,2,4-triazoles and benzoxazoles as potent antimicrobial and analgesic agents. Eur. J. Med. Chem. 2013;62:410–415.
13. Schneider G, Fechner U. Computer-based de novo design of druglike molecules. Nature Reviews Drug Discovery. 2005;4(8): 649-663.
14. Peerzade N, Jadhav A, Shravan Y, Bhikaji BR, Anantrao KA, Dnyandeo VB. Synthesis, Docking, *in silico* ADMET and Pharmacological Evaluation of Some N-acetyl Pyrazole and Quinoline Conjugates. Letters in Drug Design & Discovery. 2020;17(8):1015-1026.

15. Mallinson TE. A review of ketorolac as a prehospital analgesic. Journal of Paramedic Practice. 2017;9(12):522-526.
16. El-Shoukrofya Heba MS, El Razika Omaima AA, Wafaa Aida MA, El-Ashmawy EB. Pyrazoles containing thiophene, thienopyrimidine and thienotriazolopyrimidine as COX-2 selective inhibitors: Design, synthesis, *in vivo* anti-inflammatory activity, docking and *in silico* chemo-informatic studies Bioorganic Chemistry. 2019;85:541-557.
17. Bandgar BP, Adsul LK, Chavan HV, Jalde SS, Shringare SN. Synthesis, biological evaluation, and docking studies of 3-(substituted)- aryl-5-(9-methyl-3-carbazole)-1H-2-pyrazolines as potent antiinflammatory and antioxidant agents. Bioorganic & Medicinal Chemistry Letters. 2012;22(18):5839-5844.
18. Wiseman LR, Mc Tavish D. Formestane. A review of its pharmacodynamic and pharmacokinetic properties and therapeutic potential in the management of breast cancer and prostatic cancer. Drugs. 1993;45(1):66-84.
19. Khaled RA, Abdellatifab Eman KA, Abdelalla Madlen B, Labiba Wael AA, Fadalya Taha HZ. Synthesis of novel halogenated triarylpyrazoles as selective COX-2 inhibitors: Anti-inflammatory activity, histopatholgical profile and *in-silico* studies. Bioorganic Chemistry. 2020;105:104418.
20. Frisch MJ, Trucks GW, Schlegel HB, Scuseria GE, Robb MA, Cheeseman JR, et al. Gaussian 09, Revision A.02, Gaussian, Inc., Wallingford CT; 2009.
21. Bouanane X, Bounekhel M, Elkolli M, Abrigach F, Khoutoul M, Bouyala R, et al. Synthesis, structural, catecholase, tyrosinase and DFT studies of pyrazoloquinoxaline derivatives. Journal of Molecular Structure. 2017;1139:238–246.
22. Cheng F, Li W, Zhou Y, Shen J, Wu Z. admet SAR: A Comprehensive Source and Free Tool for Assessment of Chemical ADMET Properties. Journal of Chemical Information and Modeling. 2012;52(11):3099-3105.
23. Shilpa T, Varalakshmi Devi K. Molecular docking and synthesis of 5- acetylpyrimidine 2, 4, 6 trione based chalcones. World Journal of Pharmaceutical Research. 2017;7(03):664-673.
24. Seeliger D, De Groot BL. Conformational transitions upon ligand binding: holo-structure prediction from apo conformations. PLo Scomputational Biology. 2010;6:e1000634.
25. Lucido MJ, Orlando BJ, Vecchio AJ, Malkowski MG. Crystal Structure of Aspirin-Acetylated Human Cyclooxygenase-2: Insight into the Formation of Products with Reversed Stereochemistry. Biochemistry. 2016;55(8): 1226-1238.
26. Delano WL. The PyMOL Molecular Graphics System. De-Lano Scientific, San Carlos, CA, USA; 2002.
27. Moniruzzaman Mohammed JH, Mohammad NU, Amrin A, Tareq M. Quantum chemical, molecular docking, and ADMET predictions of ketorolac and its modified analogues. Biomed J Sci & Tech Res. 2018;11(5):8723-8729.
28. Bhuvaneswaria S, Umadevia M, Vanajothi R. Effects on anti-inflammatory, DNA binding and molecular docking properties of 2-chloroquinolin-3-yl-methylene-pyridine/pyrazole derivatives and their palladium (II) complexes. Bioorganic & Medicinal Chemistry Letters. 2020;30(21):127593.
29. Kohn W, Becke AD, Parr RG. Density functional theory of electronic structure. J. Phys. Chem. 1996;100:12974.
30. Parr RG, Pearson RG. Absolute hardness: companion parameter to absolute electronegativity. J. Am. Chem. Soc. 1983;105:7512.
31. Parr RG, Szentpaly LV, Liu S. Electrophilicity index. J. Am. Chem. Soc. 1999;121:1922.
32. Antoine D, Olivier M, Vincent Z. Swiss ADME: A free web tool to evaluate pharmacokinetics, druglikeness and medicinal chemistry friendliness of small molecules. Scientific Reports. 2017;7(1):42717.
33. Daina A, Zoete VA. BOILED-Egg to predict gastrointestinal absorption and brain penetration of small molecules. Chem Med Chem. 2016;11:1117–1121.
34. Testa B, Kraemer SD. The Biochemistry of Drug Metabolism – An Introduction. Chemistry & Biodiversity. 2007;4:257-405.
35. Van Waterschoot RAB, Schinkel AH. A critical analysis of the interplay between cytochrome P450 3A and P-glycoprotein: recent insights from knockout and transgenic mice. Pharmacological Reviews. 2011;63:390–410.
36. Wolf CR, Smith G, Smith RL. Pharmacogenetics. British Medical Journal. 2000;320:987.
37. Hollenberg PF. Characteristics and common properties of inhibitors, inducers, and activators of CYP enzymes. Drug Metab. Rev. 2002;34:17–35.
38. Huang SM. New era in drug interaction evaluation: US Food and Drug Administration update on CYP enzymes, transporters, and the guidance process. J. Clin. Pharmacol. 2008;48:662–670.

39. Lipinski CA, Lombardo F, Dominy BW, Feeney PJ. Experimental and computational approaches to estimate solubility and permeability in drug discovery and development settings. Adv. Drug. Deliv. Rev. 2001;46:3–26.
40. Egan WJ, Merz KM, Baldwin JJ. Prediction of Drug Absorption Using Multivariate Statistics. J. Med. Chem. 2000;43:3867–3877.
41. Ghose AK, Viswanadhan VN,. Wendoloski JJ. A knowledge-based approach in designing combinatorial or medicinal chemistry libraries for drug discovery. 1. A qualitative and quantitative characterization of known drug databases. J Comb. Chem. 1999;1:55–68.
42. Veber DF. Molecular properties that influence the oral bioavailability of drug candidates. J. Med. Chem. 2002;45:2615–2623.
43. Muegge I, Heald SL, Brittelli D. Simple selection criteria for drug-like chemical matter. J. Med. Chem. 2001;44:1841–1846.
44. Solis W. Minimization by random search techniques. Mathematics of Operations Research. 1981;6(1):19-30.
45. Moniruzzaman Hoque MJ, Ahsan A, Hossain MB. Molecular docking, pharmacokinetic, and DFT calculation of naproxen and its degradants. Biomedical Journal of Scientific & Technical Research. 2018;9:5.